Journal of Cell Science 104, 353-363 (1993)
Printed in Great Britain © The Company of Biologists Limited 1993

Quantitative analysis of stress fiber orientation during corneal wound contraction

W. Matthew Petroll, H. Dwight Cavanagh, Patricia Barry, Peter Andrews and James V. Jester*

Department of Ophthalmology, The University of Texas Southwestern Medical Center at Dallas, 5323 Harry Hines Blvd., Dallas, TX 75235-9057, USA

*Author for correspondence

SUMMARY

Previous studies of actin and actin-binding proteins in corneal myofibroblasts suggest the development of a contractile apparatus composed, in part, of F-actin micro-filament bundles, i.e. stress fibers. To better understand the mechanics of wound contraction and the relationship between microfilament bundles and wound closure, we have analyzed the spatial and temporal organization of stress fibers during the process of corneal wound healing. Rabbit corneas (26 eyes) received 6 mm full-thickness, central incisions and were studied at various times for F-actin organization using en bloc (whole cornea) staining with FITC-phalloidin, as well as conventional histological techniques. 3-D datasets (*z*-series of 40 en face optical sections, 1 μm steps) were collected using the Biorad MRC-600 laser scanning confocal microscope at various regions within the wound. At 7 days, 3-D analysis showed randomly oriented, interconnected F-actin filament bundles (stress fibers). Between 7 and 28 days, stress fibers appeared to organize gradually into planes parallel to the wound surface, with a large population achieving a final orientation nearly parallel to the long axis of the wound. Using Fourier Transform analysis techniques, an orientation index (OI) was calculated to quantitate global fiber orientation at each time point. Analysis of variance demonstrated a significant change ($P < 0.001$) in overall stress fiber orientation from a random distribution at day 7 to an alignment more parallel to the lateral wound borders at day 28. Overall, these data suggest that stress fibers undergo temporal changes in spatial organization that correlate with wound closure, and that wound closure does not involve the development of previously described contractile or tractional forces aligned directly across the wound.

Key words: stress fibres, myofibroblasts, wound contraction, confocal microscopy

INTRODUCTION

Previous studies in skin and cornea have shown that wound healing involves the transformation of adjacent tissue fibrocytes to myofibroblast-like cells which contain prominent microfilament bundles (stress fibers) and exhibit *in vitro* contractile responses to pharmacological agents (Gabbiani et al., 1971, 1972; Jester et al., 1987; Luttrull et al., 1985; Majno et al., 1971). More recently, myofibroblasts were shown to develop a putative contractile apparatus composed in part of intracellular F-actin microfilament bundles, α-actinin and non-muscle myosin, which was linked to extracellular fibronectin fibrils by the fibronectin membrane surface receptor, $\alpha_5\beta_1$ integrin (Garana et al., 1992; Welch et al., 1990). Although the development of a contractile apparatus temporally correlates with wound contraction, the mechanism by which actin and/or stress fibers generate tension within the wound is not known.

The development of stress fibers within wound-healing fibroblasts suggests the involvement of a sarcomeric-like shortening of the actin filament bundles in wound contraction (Byers et al., 1984; Majno et al., 1971). Although shortening of stress fiber bundles in intact cells has not been observed (Burridge, 1981), studies by Gabbiani identifying the presence of smooth muscle-specific α-actin further supports the role of a stress fiber-mediated, smooth muscle-like contractile mechanism (Darby et al., 1990; Desmouliere et al., 1992). As proposed by Welch et al. (1990) these contractile forces may be generated by interactions between intracellular actin and extracellular fibronectin as mediated by $\alpha_5\beta_1$ integrin, resulting in "pulling in" of newly synthesized extracellular matrix. In a contractile model, the force generated by actin filaments would be directed along the axis of the microfilament bundle. Characterizing the changes in microfilament bundle organization during healing may therefore provide insights into the mechanism of wound contraction and the role of F-actin.

The purpose of this study was to analyze the 3-D spatial orientation of the microfilament bundles during the wound-

healing process following full-thickness, incisional injury to the rabbit cornea. We report that the stress fibers develop a unique pattern of alignment parallel to the long axis of the incisional wound. In the center of the wound there is a change in the organizational pattern from a random orientation to an alignment parallel to the long axis, which temporally correlates with reduction in wound gape across the short axis of the wound.

MATERIALS AND METHODS

Animal wound model

Twenty-six New Zealand albino rabbits (2.5-3.0 kg) received 6 mm full thickness central corneal wounds in one eye. Rabbits were anesthetized using Rompun (2 mg/kg body weight) and Ketamine (30 mg/kg body weight). Animals were positioned underneath a Weck operating microscope and a partial-thickness incision was made using a diamond knife with a micrometer adjustment (Rhein Medical, Inc.) set to 90% of central corneal thickness, as measured by an ultrasonic pachymeter (Sonagauge, Corneo-gage III). A sterile no. 11 Bard Parker blade was then used to finish the cut through the posterior cornea, with care taken not to disturb the lens capsule or iris. In 6 rabbits, in vivo measurements of wound gape were made using the tandem scanning confocal microscope (TSCM) at 3, 7, 10, 14 and 28 days after injury. In addition, 4 animals were killed at each time point: one for light microscopy (LM), one for epi-immunofluorescence microscopy (FM), and two for laser confocal microscopy (LCM).

Tandem scanning confocal microscopy (TSCM)

TSCM allows for high-resolution, in vivo imaging of the cornea and other tissues. For examination of in vivo histology and measurement of wound gape, animals were scanned at sequential time points using a modified TSCM (Tandem Scanning Corp., Reston, VA) with a 24× surface contact objective (NA = 0.6, WD = 1.5 mm). The design of this microscope has been described previously (Jester et al., 1991, 1992a,b; Petroll et al., 1992). Images were detected using a DAGE SIT 66 video camera and recorded on Super VHS tape (JVC, model BR-S611U). Rabbits were anesthetized using Rompun (2 mg/kg body weight) and Ketamine (30 mg/kg body weight), and two drops of Tetracaine were applied for topical anesthesia. After applanating the objective to the corneal surface, the beginning of an incision was identified. The position of the focal plane was maintained at the level of the basal lamina using the mechanical *z*-axis control drive on the objective. Wound gape was measured by placing a transparency with a grid of 10 μm spacing over the screen (Jester et al., 1992b). Measurements were taken in the center, of the wound, 1 mm nasally and 1 mm temporally from the center, and an average wound gape was determined.

Light and electron microscopy

Following killing, selected corneas were fixed by anterior chamber perfusion with 2.5% glutaraldehyde in 0.1 M phosphate buffer, pH 7.3, for 10 minutes. Corneas were then removed and fixed overnight. For light microscopy, a block including the central portion of the wound was then dehydrated and embedded in glycolmethacrylate, cut in cross-section (4 μm thick) on a Reichert-Jung 2050 microtome, and stained with hemotoxylin and eosin (H&E). For transmission electron microscopy (TEM), tissue blocks were washed 3 times in 0.1 M phosphate buffer, pH 7.2, after overnight fixation. Tissue was then post-fixed with 1% osmium tetroxide (O_sO_4) in 0.1 M phosphate buffer for 1 hour, dehydrated in graded ethanols, embedded in Spur resin, and polymerized overnight in a 60˚C oven. Ultramicrotome sections were cut and stained with uranyl acetate and lead acetate, and examined on a JEOL 1200 EX TEM.

Epi-immunofluorescence microscopy

Selected corneas were processed for study of F-actin distribution using wide-field epi-fluorescence microscopy (FM). After killing, the wound area was blocked out, cut in half (perpendicular to long axis), embedded in OCT compound and frozen in liquid nitrogen. One block was oriented such that the tissue section cross-sected the corneal wound, whereas the other was oriented parallel to the wound surface, i.e. en face (Fig. 1). Specimens were cut into 7 μm sections and stained for 40 minutes with phalloidin-FITC (Molecular Probes), which binds to F-actin (Barak et al., 1980). To identify cell nuclei, selected sections were also stained with propidium iodide as described by Jones and Senft (1985).

Laser confocal microscopy (LCM)

Selected corneas were studied for F-actin distribution and organization using LCM (Biorad MRC-600). After killing, corneas were fixed by a 3 minute anterior chamber perfusion with 1% paraformaldehyde in phosphate-buffered saline, pH 7.2 (Garana et al., 1992). The wound area was then blocked out and cut in half (perpendicular to long axis) and each half was labelled, en bloc, with 200 μl of 1.7 μM (50 i.u./ml) phalloidin-FITC in 1% DMSO and 5% Triton X-100 in phosphate buffer for 3 hours.

LCM permits thin en face optical sectioning through the cornea (see Fig. 1). A stack of en face optical sections (*z*-series) can be acquired by changing the position of the focal plane in small steps. Both single 2-dimensional images of 3-5 μm thick optical sections (768 × 512 pixels, 256 grey levels), and 3-dimensional datasets (*z*-series of 40 en face optical sections, 384 × 256 pixels per image, 1 μm steps) of thinner optical sections (1-2 μm) were acquired. Both the LCM and en face FM microscopy data presented were taken between 20 and 80 μm below the anterior surface of the wound, since this was the deepest penetration into the tissue blocks which could be obtained using LCM. In all en face FM and LCM images, the wound was aligned such that the long axis was oriented vertically, and the short axis horizontally. At least one *z*-series and two 2-D images were obtained from each wound; centered between the lateral wound margins, near the middle of the long dimension of the wound. In order to assess regional differences in the wound-healing response, an additional

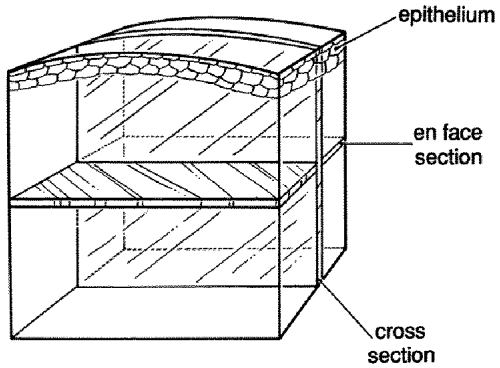

Fig. 1. Sketch demonstrating the relationship between cross and en face orientations in the cornea.

four to five 2-D images were obtained near the ends and lateral edges of the wounds at each time point.

Data analysis

Images obtained from the LCM were transferred to a Silicon Graphics 4D/35G computer, where the ANALYZE software package (Mayo Medical Ventures) was used for display and analysis (Robb et al., 1989; Robb and Barillot, 1989). In order to evaluate the global organizational changes in F-actin, we applied a Fourier Transform (FT) analysis procedure previously used to identify collagen fiber orientation in other tissues (Chaudhuri et al., 1987; Kronick and Sacks, 1991; Yang et al., 1987). The FT of a 512 × 512 or 256 × 256 pixel area within a 2-dimensional image was calculated using ANALYZE, the magnitude spectrum was shifted to center the zero frequency value $\{F(0,0)\}$, and normalized by setting $F(0,0)$ to the maximum grey value (255). The relative strength of different angle bands within the FT is a global indicator of the relative number and magnitude of fibers oriented at 90 degrees to that angle in the original image. Using polar coordinates (r, φ), line averages ($I(\varphi)$ from the center to the periphery (i.e. r = 4 to 256) were calculated at 2 degree intervals from the normalized FT magnitude spectrum. Points close to the center (r < 4) were excluded from the line averages, since they represent low-frequency information (such as shading), which is not of interest. A 2-dimensional "orientation index" (OI) was then used to quantitate the degree of orientation along the long axis of the wound from the FT line averages, using the equation (Kronick and Sacks, 1991):

$$\mathrm{OI} = \{2(\cos^2\varphi) - 1)100\%,$$

where

$$\cos^2\varphi = \frac{\int_{-\pi/2}^{\pi/2} I(\varphi)\cos^2\varphi d\varphi}{\int_{-\pi/2}^{\pi/2} I(\varphi) d\varphi}$$

and $\varphi = 0$ is the x axis in the FT image, corresponding to the long axis of the wound (y axis) in the original image. The OI has a value of 0% for a completely random distribution of fibers, 100% for an alignment of all fibers parallel to the long axis of the wound, and −100% for a fiber alignment perpendicular to the wound. Because the OI is based on the dimensionless $\cos^2\varphi$ value, it is dependent on the relative magnitude of the line averages, not the absolute magnitudes. Thus, no additional normalization for differences in the overall number or intensity of stress fibers between images is necessary (Chaudhuri et al., 1987). However, the line average data presented graphically have been normalized for clarity of display. The OI was calculated for the highest quality LCM images, which were centered within the wound, with the constraint that no more than 2 images from a single z-series were used (n = 6 for days 7, 14 and 28, n = 4 for day 10).

Statistical evaluation

All statistics were calculated using the SYSTAT software package (SYSTAT, Inc.). A one-sided Student's t-test was used to determine if the OI value at each time point was significantly greater than zero. An analysis of variance was performed and the Tukey Test was used to compare the OI at different time points to each other. Linear regression analysis was used to determine the relationship between temporal changes in OI and wound gape.

RESULTS

General observations

The initial wound-healing response observed by in vivo TSCM and standard histology at day 3 includes the formation of a fibrin clot, migration of epithelium into the anterior portion of the wound, and the initial migration of adjacent tissue fibrocytes into the anterior wound borders. By day 7, myofibroblasts have migrated into the anterior portion of the wound, while the fibrin clot remains in the posterior region (Fig. 2A). No regular arrangement or layering of the myofibroblasts is apparent at this time. By day 10, the myofibroblasts have completely replaced the fibrin clot, and filled the wound space. At 14 and 28 days, histological cross-sections show that the myofibroblasts are organized into layers parallel to the anterior corneal surface (Fig. 2B). TEM demonstrates that stress fibers can be observed in the myofibroblasts as early as 7 days after injury, and are still present 28 days after injury (Fig. 2C).

Comparison of FM and LCM

In the rabbit model, both the cross and en face FM sections show intense F-actin staining of the myofibroblasts within the wound from 7 to 28 days after surgery, and a progressive increase in F-actin organization during wound healing. The cross-sections (oriented as shown in Fig. 1) show F-actin to be randomly distributed within the wound at 7 days. By 14 days, it appears that the fibroblasts are organized into layers parallel to the wound surface (Fig. 3A, B). Based on the propidium iodide staining of cell nuclei, it is evident that this increase in staining is due to increased expression of F-actin by the fibroblasts within the wound, and not simply an increase in cell numbers. If viewed alone, the cross-sectional view of these layers could lead to the interpretation that the stress fibers are oriented directly *across* the wound, i.e. perpendicular to the lateral wound margins. The 14-day en face data (oriented as in Fig. 1) reveal that the stress fibers lie nearly parallel to the en face plane, as demonstrated by the ability to distinguish thin stress fiber bundles (Fig. 3C, arrows). However, in contrast to what is suggested from the cross-sectional data, the stress fibers are oriented *parallel* to the long axis of the wound. This is exactly opposite to the fiber orientation suggested from cross-sectional observations alone, and demonstrates the importance of studying 3-dimensional systems with 3-dimensional techniques. The cross-sectional data are misleading because the myofibroblasts organize into layers which have the appearance of stress fibers spanning across the wound when viewed from the side.

The F-actin distribution observed using in situ LCM of en bloc-stained corneal tissue is similar to that seen using FM. LCM images at 14 days show prominent stress fibers, most of which are also oriented nearly parallel to the long axis of the wound (Fig. 3D). However, the improved optical sectioning of LCM reduces the amount of out-of-focus information contributing to the image, and allows the acquisition of 3-D datasets in whole tissue, which can provide improved insight into 3-D stress fiber organization. Furthermore, LCM eliminates orientation artifacts associated with physically sectioning the tissue. Thus further analysis was focussed on the LCM images.

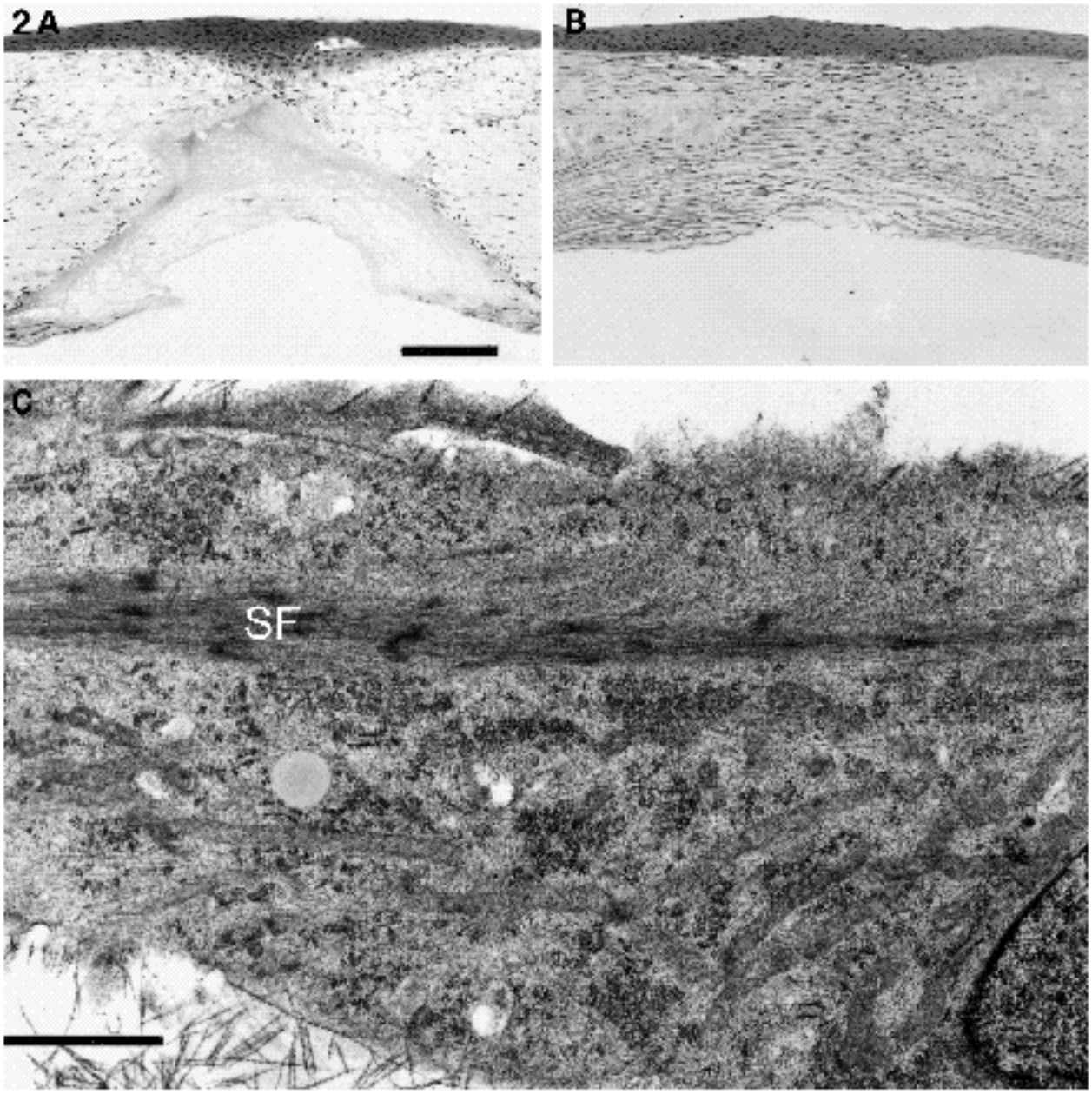

Fig. 2. (A) Histological cross-section of full-thickness incision 7 days after surgery. Myofibroblasts have migrated into the anterior portion of the wound, although the fibrin clot remains in the posterior region. No regular arrangement or layering of the myofibroblasts is apparent at this time. (B) Histological cross-section of full thickness incision 28 days after surgery. At 28 days, the myofibroblasts are clearly organized into layers parallel to the anterior corneal surface. Note that the thickness of the wound (anteroposterior height) has decreased significantly since day 7. (C) Transmission electron microscopy of a stress fiber (SF) within a myofibroblast 28 days after injury. Bars: A, 200 μm; C, 1 μm.

Temporal organization of F-actin

Differences in the regional healing response as reflected in stress fiber organization were observed in this study. In general, the stress fibers at the lateral edges of the wounds showed more alignment with the long axis of the wound as compared to the center of the wound, as often dramatized by the presence of thick cable-like stress fibers along the wound margins (Fig. 4, arrows). Furthermore, the beginning and end of the incisional wounds healed faster than the central regions. Corresponding with the accelerated healing in these areas was an earlier shift in the alignment of the stress fibers toward the long axis of the wound. To avoid the potential sampling problems associated with these regional variations in healing, the 3-D analysis of fiber orientation was performed only on images centered between the lateral wound margins, near the middle of the long dimension of the wound. It should be noted that the analysis was limited to images from the anterior 80 μm of the

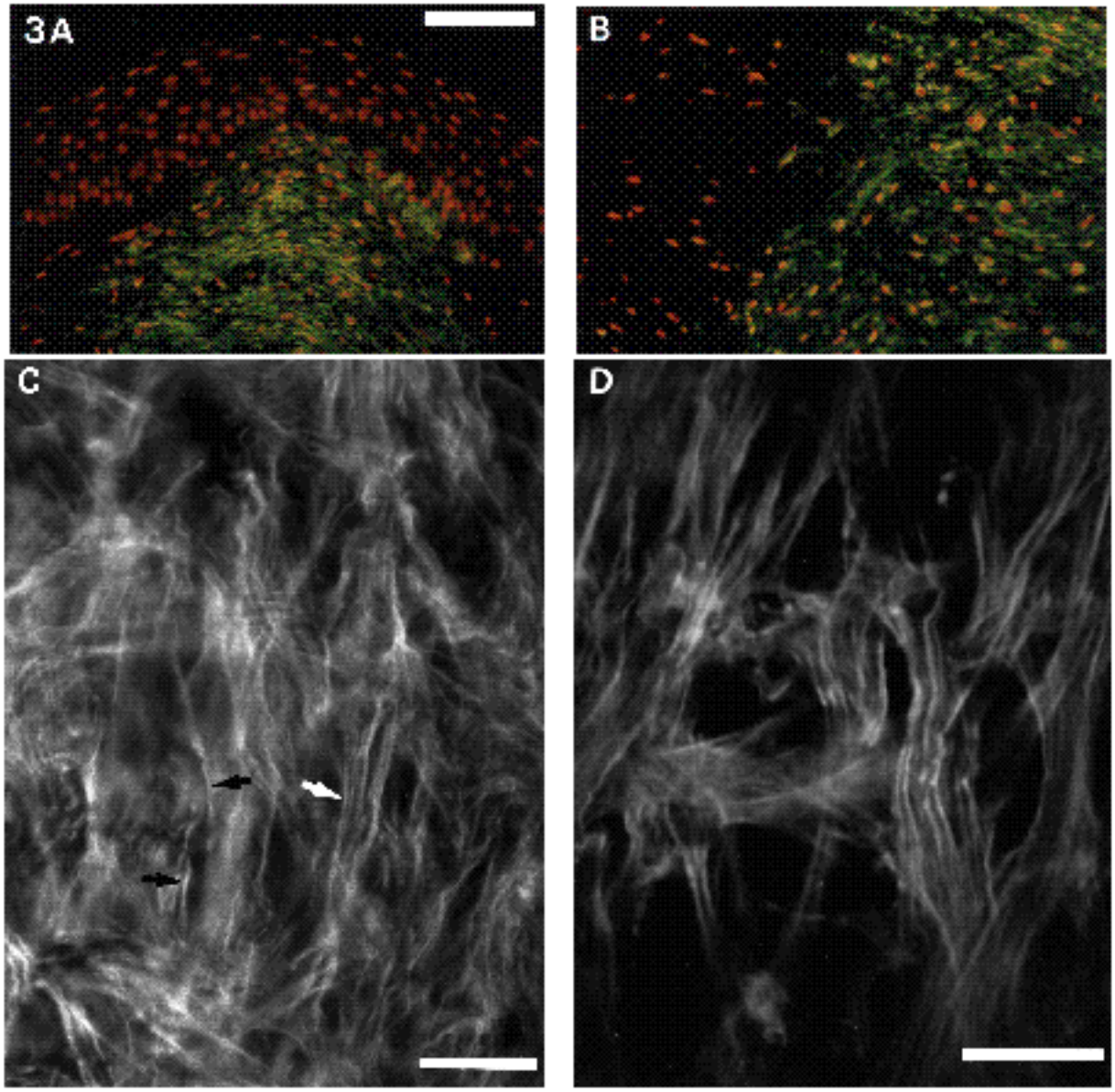

Fig. 3. (A) Low-magnification cross-section labelled for F-actin (green) and propidium iodide (red) showing light cortical F-actin staining of the epithelium, and intense staining of the myofibroblasts which have migrated into the wound. (B) Image from a different area in the same cross-section as A. It appears in both A and B that the fibroblasts are organized into layers parallel to the wound surface. (C) A 14-day en face section, which suggests that the stress fibers (arrows) are oriented parallel to the long axis of the wound. (D) The F-actin distribution observed using in situ LCM of en bloc-stained corneal tissue at 14 days after injury. The improved optical sectioning of LCM reduces the amount of out-of-focus information contributing to the image as compared to C. Bars: A, 100 μm; C,D, 25 μm.

wound, although en face sections from deeper within the wound suggest that similar temporal changes in stress fiber alignment occur at all levels.

At 7 days, the 3-D LCM data suggest that F-actin is distributed into randomly oriented microfilament bundles (i.e. stress fibers) at various tissue depths below the corneal epithelium (Fig. 5). Stress fibers appear to align in parallel groups, which may correspond to individual cell processes. Between 10 and 14 days, stress fibers appear to become more aligned with the long axis of the wound. By 28 days, the 3-D organization of the stress fibers appears to be nearly parallel to the long axis of the wound (Fig. 6). At all time points, stress fibers were found to lie close to the *x-y* (i.e. en face) plane, with very small *z*-axis components. This allowed the use of 2-D orientation analysis procedures on the en face LCM images.

A sample of the quantitative analysis of fiber orientation at 10 and 28 days after injury is shown in Fig. 7. The 10-day image (Fig. 7A) appears to have stress fibers oriented at several different angles. The FT (Fig. 7B) produces a somewhat circular pattern with two angle bands at 20 and −40 degrees which appear slightly brighter than the rest, most likely corresponding to the parallel groups of stress fibers indicated by the open and closed arrows (see Fig.

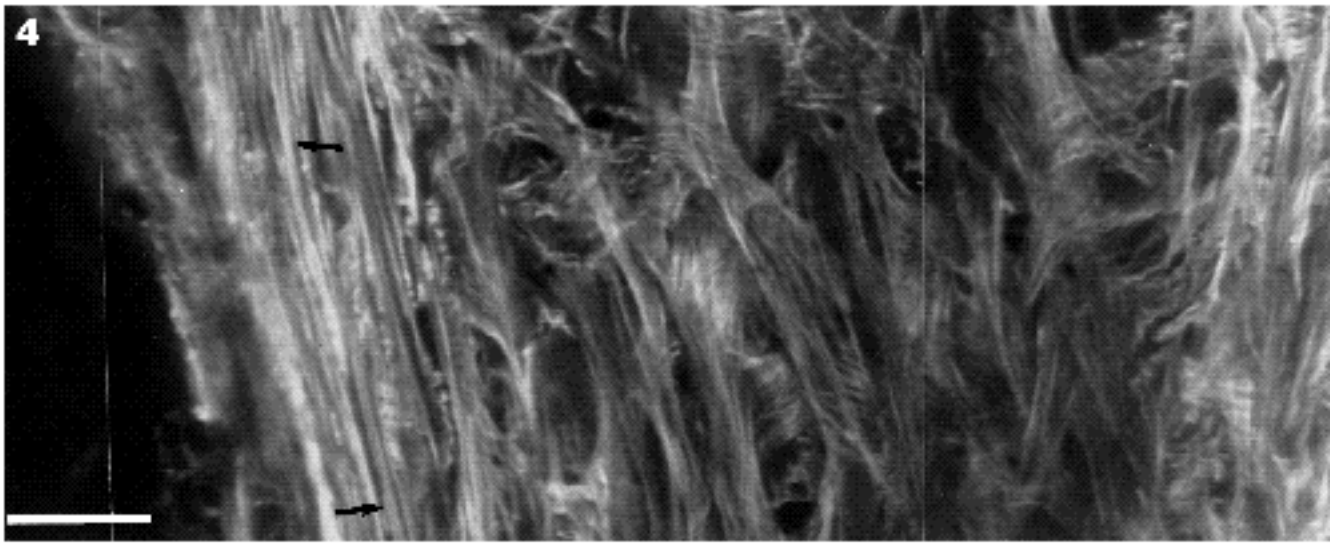

Fig. 4. A montage of LCM images demonstrating the potential sampling problems which exist in the full-thickness wound model. The stress fibers at the lateral edges of the wounds show more alignment with the long axis of the wound as compared to the center of the wound, as dramatized by the presence of thick cable-like stress fibers along the wound margins (arrows). Bar, 25 μm.

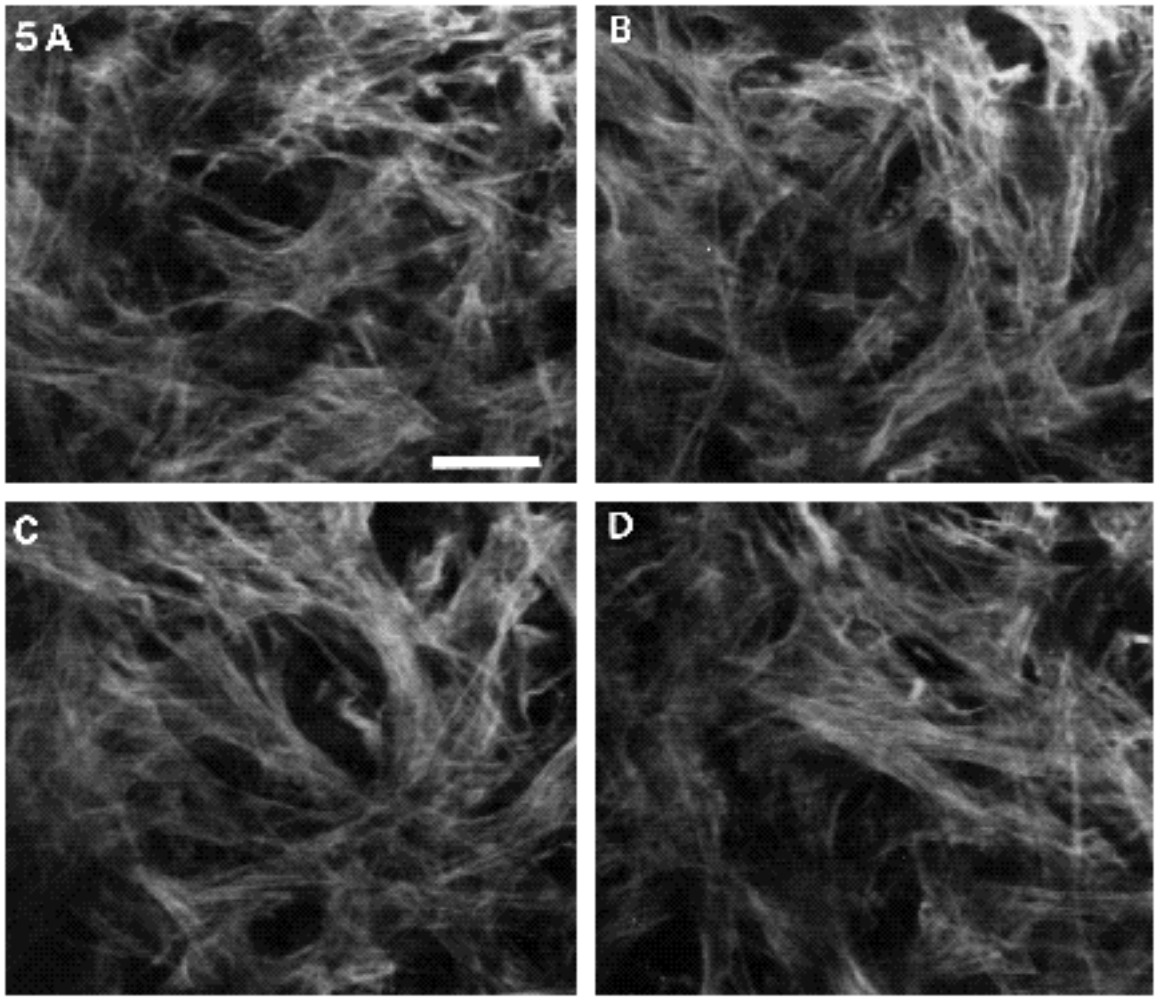

Fig. 5. LCM optical sections within a 40 μm *z*-series from a 7-day wound labeled en bloc for F-actin. Images A, B, C and D are, respectively, 10, 16, 22 and 28 μm below the bottom of the epithelial plug. Note that the F-actin microfilament bundles (i.e. stress fibers) appear to be randomly oriented. The long axis of the wound is oriented vertically. Bar, 25 μm.

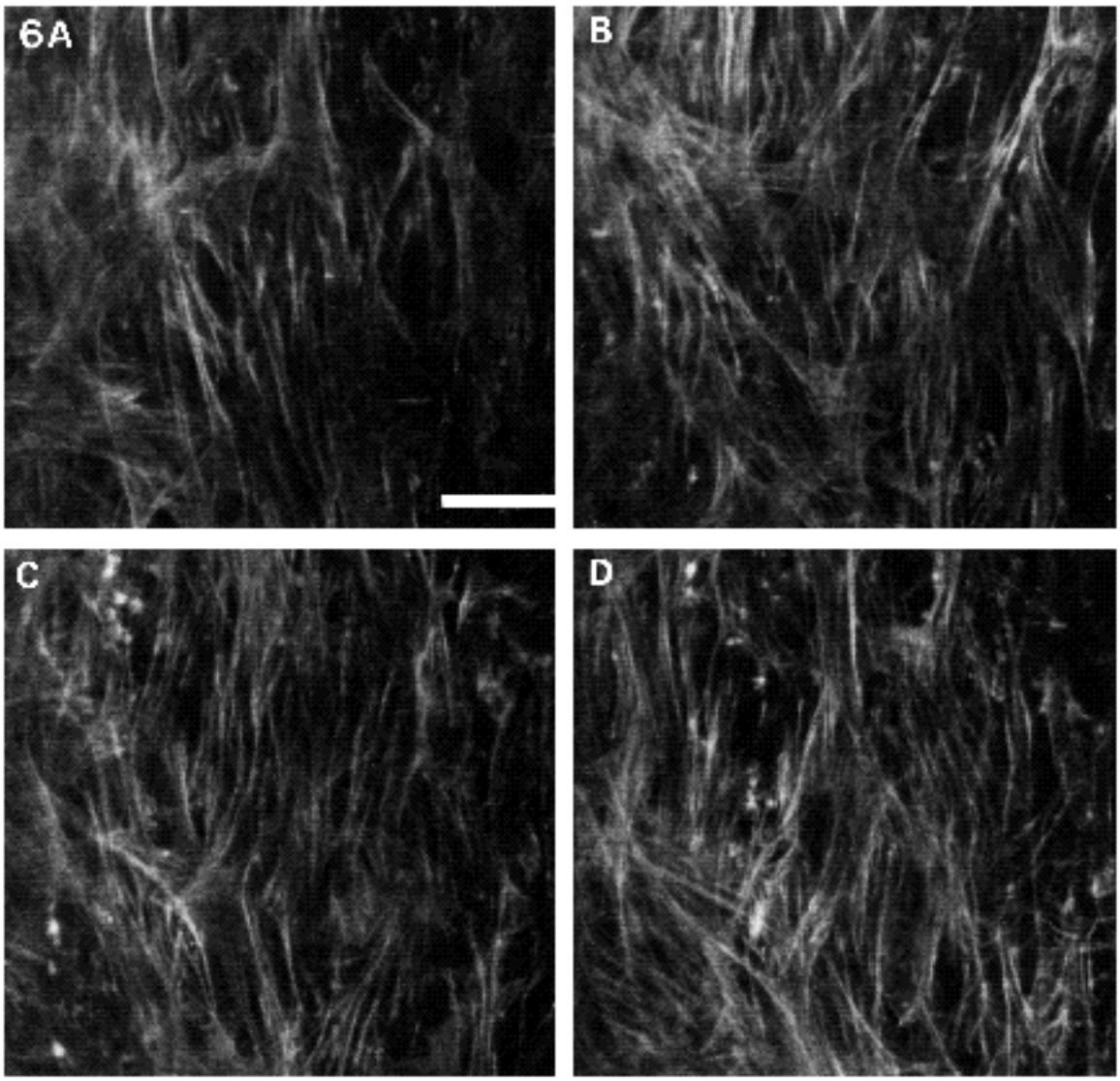

Fig. 6. LCM optical sections within a 40 μm *z*-series from a 28-day wound labeled en bloc for F-actin. Images A, B, C and D are, respectively, 10, 16, 22 and 28 μm below the basal epithelial cells. Note that the stress fibers appear to be organized predominantly along the long axis of the wound (vertically). Bar, 25 μm.

7A), respectively. This results in a line average plot with two peaks (Fig. 7C). The OI of 20% demonstrates that there is a slight overall alignment of fibers in the original image with the long axis of the wound. The day 28 image shows alignment of the fibers almost parallel to the long axis of the wound (Fig. 7D) (for demonstration purposes, an image with an alignment somewhat more dramatic than most of the day 28 images is shown). The FT produces an elliptical pattern (Fig. 7E), with the major axis at 90 degrees to the long axis of the wound. A plot of the line averages calculated from the FT shows a sharp peak near 0 degrees (Fig. 7F). The higher OI of 56% confirms that the fibers are more aligned with the long axis than in the 10-day image.

A temporal change in the angle distribution of the stress fibers was also observed, as reflected in the shape of the FT line averages (Fig. 8A). A large population of stress fibers oriented near the long axis of the wound was observed at all time points, corresponding to the central peaks in the line average plots. However, “side lobes” were observed which progressively decreased in relative magnitude over time. This is especially apparent at day 7, which suggests that two separate populations of fibers with different orientations may be present, one oriented along the wound, and one across the wound. OI calculations indicate that the stress fibers were randomly oriented at 7 days (OI = −1.6 ± s.d. 3.8%), and progressively increased in orientation to 28 days after surgery (OI = 31.4 ± 13.8%) (Fig. 8B). The OI was significantly greater than zero at 10, 14 and 28 days ($P = 0.01$), indicating non-random alignment towards the long axis of the wound. A significant increase in the OI was found between 7 and 14, and 7 and 28 days ($P < 0.001$), based on analysis of variance. Wound gape progressively decreased from 671 ± 97 μm at 3 days after

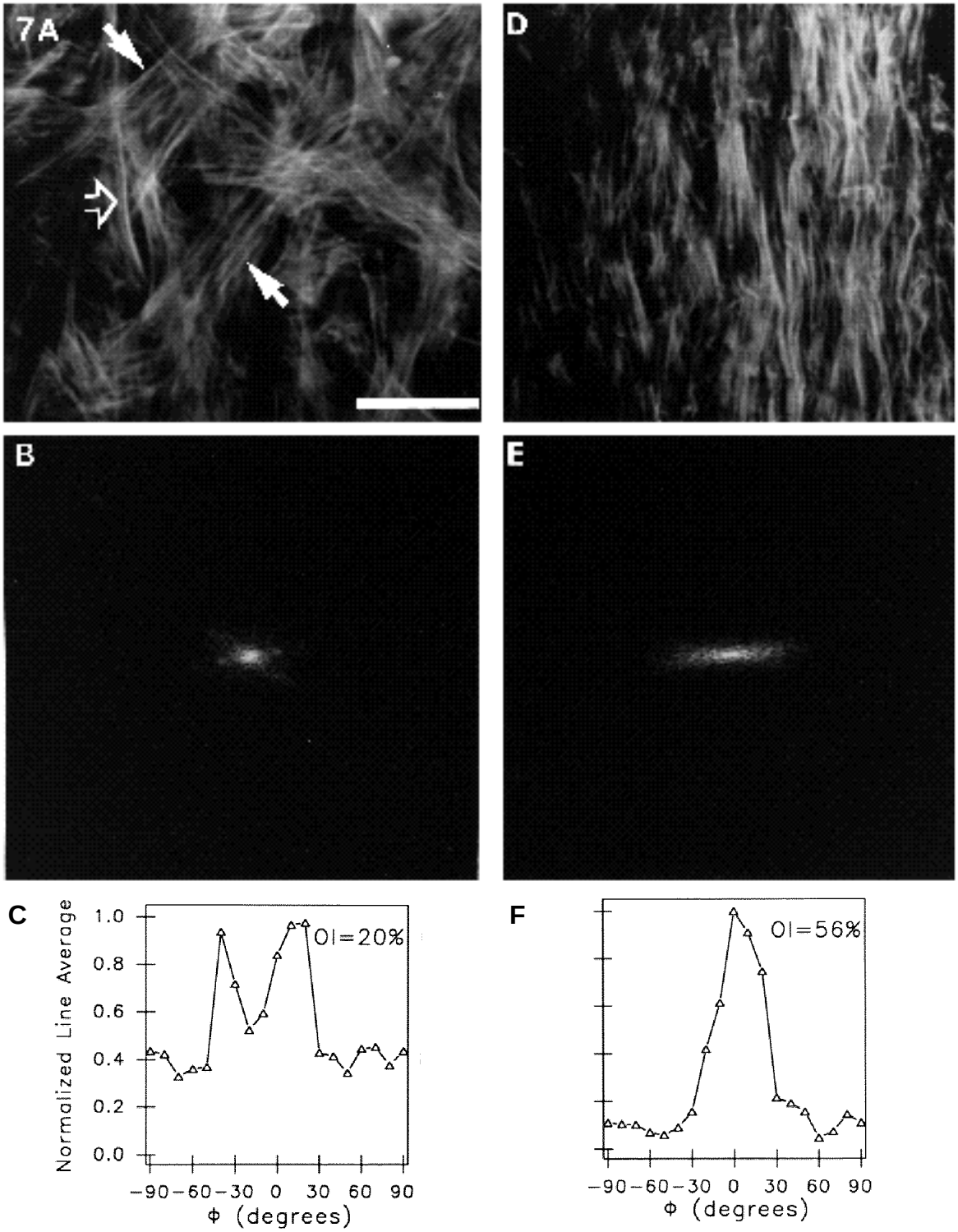

Fig. 7. Results of the analysis of fiber orientation at 10 (A, B and C) and 28 (D, E and F) days after injury. (A) The 10-day image of a corneal wound appears to show stress fibers oriented at several different angles. (B) The Fourier Transform (FT) of image A produces a somewhat circular pattern with two angle bands at 20 and −40 degrees which appear slightly brighter than the rest, most likely corresponding to the parallel groups of stress fibers indicated by the open and closed arrows, respectively (see A). (C) Line average plot of FT showing two peaks. The OI of 20% demonstrates that there is a slight overall alignment of fibers in the original image with the long axis of the wound (an OI of 0% = completely random distribution, 100% = completely parallel to long axis, −100% = completely perpendicular to the long axis). (D) The day 28 image of the corneal wound shows alignment of the fibers almost parallel to the long axis. (E) The FT produces an elliptical pattern, with the major axis at 90 degrees to the long axis of the wound. (F) A plot of the line averages of the FT shows a sharp peak near 0 degrees. The resulting orientation index (OI) of 56% confirms that the fibers are more oriented along the long axis than the 10-day image. Bar, 25 μm.

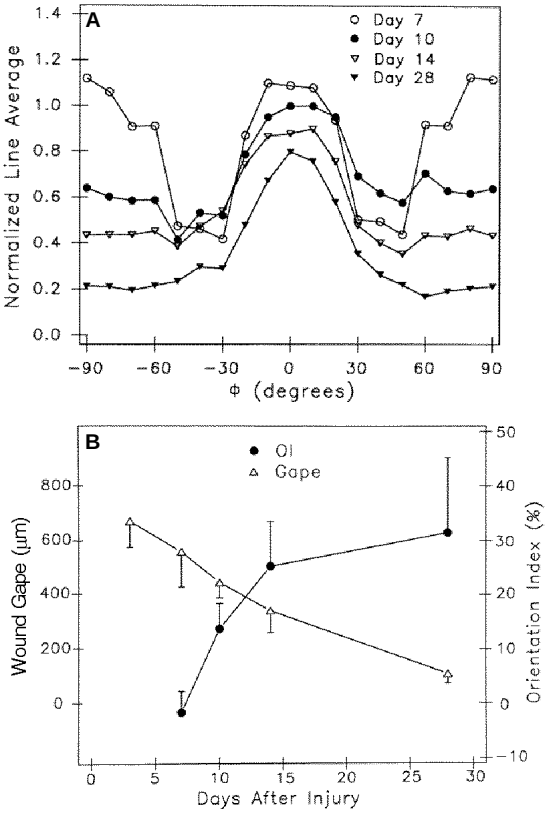

Fig. 8. (A) Temporal change in the mean angle distribution of the FT line averages. For visual clarity, the plots at day 7, 10, 14 and 28 were normalized so that the line average values at zero degrees were 1.1, 1.0, 0.9 and 0.8, respectively. A large population of stress fibers oriented near the long axis of the wound was observed at all time points, corresponding to the central peaks in the line average plots. However, "side lobes" were observed, which progressively decreased in relative magnitude over time. This is especially apparent at day 7, which suggests that two separate populations of fiber orientation may be present, one oriented along the wound, and one across the wound. (B) A plot of the overall changes in stress fiber orientation (OI) and wound gape over time (error bars represent s.d.). OI calculations indicate that the stress fibers were randomly oriented at 7 days (OI = −1.6 ± s.d. 3.8%), and progressively increased in orientation to 28 days after surgery (OI = 31.4 ± 13.8%). Wound gape progressively decreased from 708 ± 98 μm at 3 days after surgery to 130 ± 14 μm at day 28.

surgery to 108 ± 35 μm at day 28 (Fig. 8B). A significant negative correlation was found between wound gape and OI from day 7 to day 28 ($R = -0.93$, $n = 4$, $P < 0.05$).

DISCUSSION

The in vivo TSCM observations and histological data in this study show that, as in other corneal wound-healing models, the rabbit full-thickness incisional wound heals through fibrosis and progressive wound contraction (Garana et al., 1992; Jester et al., 1987). TEM confirms that prominent F-actin filament bundles (stress fibers) develop within the myofibroblasts during wound healing. Thus, the rabbit

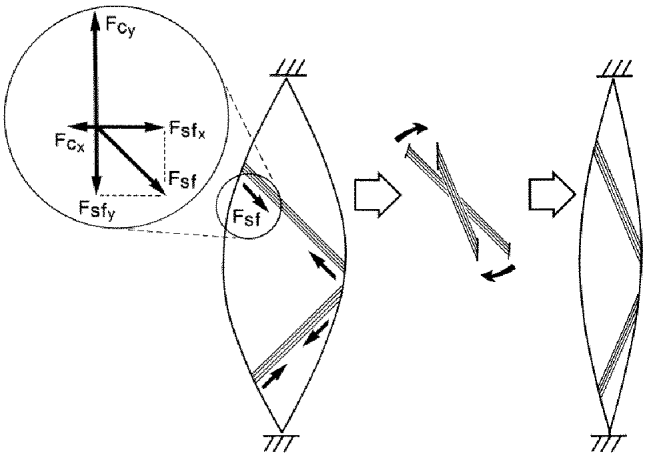

Fig. 9. A simplified sketch of one possible mechanism by which stress fibers may become oriented along the long axis of the wound during contraction. In this contractile model, stress fibers generate force *parallel* to the axis of the microfilament bundle. From a biomechanical standpoint the axial force vector (F_{sf}) can be broken down into two components, one oriented across the wound ($F_{sf,x}$) and one oriented parallel to the wound ($F_{sf,y}$). Since after incisional injury the greatest increase in wound gape occurs across the wound, there is much less resistance to shortening of wound gape across the wound than along the wound ($F_{cy} >> F_{cx}$). Therefore, during contraction stress fibers tend to twist *across* the wound as they contract in response to the differences in resistance.

incisional wound model has the same healing characteristics as those used for previous healing studies in skin and corneal tissue.

Three-dimensional LCM analysis of in situ labeled corneal wounds from the rabbit shows that the F-actin microfilament bundles develop a unique organizational pattern during wound repair. As demonstrated by the quantitative analysis of stress fiber orientation, this temporal organization involves a change in the orientation of stress fibers from a random pattern to an alignment parallel to the long axis of the wound. During the early phase of wound healing (day 7) there appears to be a small population of stress fibers in the center of the wound that is organized across the short axis (see Fig. 8A). However, later in wound healing, presumably as tension within the wound increases, this population appears to disappear. The change in organization temporally correlates with wound contraction as measured by the reduction in wound gape across the short axis of the wound. Since the greatest wound gape and hence the greatest wound contraction occurs across the short axis of the wound, the preferential alignment of the microfilament bundles along the long axis of the wound appears to conflict with a traditional contractile mechanism where the force necessary to contract the wound would be provided by microfilament bundles oriented across the short axis of the wound (Majno et al., 1971).

Although stress fibers may not be organized across the wound, a contractile model may still be important in the generation of contractile forces across the short axis of the wound and therefore play a role in wound contraction (Fig. 9). In such a model, microfilament bundles would generate

a force vector (F_{sf}) running parallel to the axis of the stress fibers, which can be broken down into two components: one oriented across the wound ($F_{sf,x}$) and one oriented parallel to the wound ($F_{sf,y}$). Since after incisional injury the greatest increase in wound gape occurs across the wound, we propose that there is less resistance to shortening of wound gape across the wound than along the wound ($F_{cy} >> F_{cx}$). Therefore, based on a force balance analysis, during contraction stress fibers would tend to twist across the wound as they contract in response to the differences in resistance (anisotropy). This process would result in closure of the wound, as well as a more parallel orientation of the fibers with the long axis of the wound, comparable to the tightening of a shoelace.

Alternatively, wound contraction may be a consequence of the forces generated during stress fiber bundle formation. As suggested by Burridge (1981), this process could be influenced by the same anisotropy within the wound as described above. Actin microfilaments may be recruited into a developing bundle along the path of least resistance, resulting in an alignment of the bundles along the axis of greatest tension. On the basis of this model for stress fiber formation, one would expect lateral "pulling in" of adjacent microfilaments as bundles develop parallel to the long axis of the wound. This lateral movement of microfilaments could play a role in the process of wound contraction.

More recently, it has been suggested that wound contraction is mediated by fibroblast locomotion, in which the force exerted by a cell to elongate and extend along a substratum is balanced by an opposite, tractional force exerted on the matrix (Harris et al., 1981; Harris, 1982; Rudolph et al., 1992; Stopak et al., 1985). Such tractional forces have also been implicated in the contraction of 3-D collagen gels, in which stress fibers are not prominent (Grinnell and Lamke, 1984; Grinnell et al., 1989; Guidry and Grinnell, 1985; Harris et al., 1981). On the basis of this observation, it has been suggested that stress fibers do not play a role in contraction, but may instead develop at the end of contraction as a transitional stage prior to cell migration out of the wound (Rudolph et al., 1992). The data from the present study are in direct contradiction with the proposed tractional model of wound contraction. Fibroblasts migrated into the wound space and developed prominent stress fibers by 7 days after injury, whereas 80% of the observed decrease in wound gape occurred between 7 and 45 days after injury. In addition, with the exception of a small population oriented across the wound at day 7, the stress fibers are predominantly oriented with the long axis of the wound throughout the course of wound closure. This is opposite to the orientation expected from cells migrating into the wound and exerting tractional forces along their axes.

An interesting finding was that, even during the early phase of wound healing, there is a preferential organization of the microfilament bundles along the margins of the wound (Fig. 4). From a biomechanical point of view, the borders of the wound represent a unique area of maximum anisotropy where rigid stroma interfaces less rigid, newly synthesized fibrotic tissue. The preferential alignment of stress fibers parallel to this interface provides further evidence that the anisotropic properties of the wound are primarily if not solely responsible for determining the orientation of the cells and intracellular stress fibers. Clearly, additional evaluation of the 3-dimensional organization of the wound, including the specific organization of the extracellular matrix and its association with the putative contractile apparatus, is necessary to understand in vivo wound contraction on a more detailed cellular and molecular basis.

This work was supported in part by the National Eye Institute grant EY07348, Research to Prevent Blindness, Inc., and the Eleanor Naylor Dana Charitable Trust.

REFERENCES

Barak, L. S., Yocum, R. R., Nothnagel, E. A. and Webb, W. S. (1980). Fluorescence staining of the actin cytoskeletan in living cells with 7-nitrobenz-2-oxa-1,3-diazole-phallacidin. *Proc. Nat. Acad. Sci. USA* **77**, 980-984.

Burridge, K. (1981). Are stress fibers contractile? *Nature* **294**, 691-692.

Byers, H. R., White, G. E. and Fujiwara K. (1984). Organization and function of stress fibers in cells in vitro and in situ. In *Cell and Muscle Motility*, vol. 5, pp. 83-137. Plenum Press, New York.

Chaudhuri, S., Nguyen, H., Rangayyan, R. M., Walsh, S. and Frank, C. B. (1987). A Fourier domain directional filtering method for analysis of collagen alignment in ligaments. *IEEE Trans. Biomed. Eng.* **34(7)**, 509-518.

Darby, I., Skalli, O. and Gabbiani, G. (1990). α-Smooth muscle actin is transiently expressed by myofibroblasts during experimental wound healing. *Lab. Invest.* **63**, 21-29.

Desmouliere, A., Rubbia-Brandt, L., Abdiu, A., Walz, T., Machieira-Coelho, A. and Gabbiani, G. (1992). α-Smooth muscle actin is expressed in a subpopulation of cultured and cloned fibroblasts and is modulated by γ-interferon. *Exp. Cell Res.* **201**, 64-73.

Gabbiani, G., Hirschel, B. J., Ryan, G. B., Statkov, P. R. and Majno, G. (1972). Granulation tissue as a contractile organ: a study of structure and function. *J . Exp. Med.* **135**, 719-734.

Gabbiani, G., Ryan, G. B. and Majno, G. (1971). Presence of modified fibroblasts in granulation tissue and their possible role in wound contraction. *Experientia* **27**, 549-550.

Garana, R. M. R., Petroll, W. M., Herman, I., Barry, P., Andrews, P., Cavanagh, H. D. and Jester, J. V. (1992). Radial keratotomy: II. Role of the myofibroblast in corneal wound contraction. *Invest. Ophthalmol. Vis. Sci.* **33**(12), 3271-3282.

Grinnell, F. and Lamke, C. R. (1984). Reorganization of hydrated collagen lattices by human skin fibroblasts. *J. Cell Sci.* **66**, 51-63.

Grinnell, F., Nakagawa, S. and Ho, C. H. (1989). The collagen recognition sequence for fibroblasts depends on collagen topography. *Exp. Cell Res.* **182**, 668-672.

Guidry, C. and Grinnell,F. (1985). Studies on the mechanism of hydrated collagen gel reorganization by human skin fibroblasts. *J. Cell Sci.* **79**, 67-81.

Harris, A. K. (1982). Traction, and its relations to contraction in tissue cell locomotion. In *Cell Behavior*, pp. 109-134. Cambridge University Press.

Harris, A. K., Stopak, D. and Wild, P. (1981). Fibroblast traction as a mechanism for collagen morphogenesis. *Nature* **290**, 249-251.

Jester, J. V., Petroll, W. M., Andrews, P., Cavanagh, H. D. and Lemp, M. A. (1991). In vivo confocal microscopy. *J. Electron Microsc. Tech.* **18**, 50-60.

Jester, J. V., Petroll, W. M., Garana, R. M. R., Lemp, M. A. and Cavanagh, H. D. (1992a). Comparison of in vivo and ex vivo cellular structure in rabbit eyes detected by tandem scanning microscopy. *J. Microsc.* **165(1)**, 169-181.

Jester, J. V., Rodrigues, M. M. and Herman, I. M. (1987). Characterization of avascular corneal wound healing fibroblasts. New insights into the myofibroblasts. *Amer. J. Pathol.* **127**, 140-148.

Jester, J. V., Petroll, W. M., Feng, W., Essepian, J. and Cavanagh H. D. (1992b). Radial keratotomy: I. The wound healing process and measurement of incisional wound gape in two animal models using in vivo, confocal microscopy. *Invest. Ophthalmol. Vis. Sci.* **33**(12), 3283-3291.

Jones, K. H., and Senft, F. A. (1985). An improved method to determine cell viability by simulataneous staining with fluorescein diacetate - propidium iodide. *J. Histochem. Cytochem.* **33**, 77-79.

Kronick, P. L. and Sacks, M. S. (1991). Quantification of vertical-fiber defect in cattle by small angle light scattering. *Conn. Tiss. Res.* **27**, 1-13.

Luttrull, J., Smith, R. and Jester, J. (1985). In vitro contractility of avascular corneal wounds in rabbit eyes. *Invest. Ophthalmol. Vis. Sci.* **26**, 1449-1452.

Majno, G., Gabbiani, G., Hirschel, B. J., Ryan, G. B. and Statkov, P. R. (1971). Contraction of granulation tissue in vitro: similarity to smooth muscle. *Science* **173**, 548-550.

Petroll, W. M., Cavanagh, H. D., Lemp, M. A., Andrews, P. M. and Jester, J. V. (1992). In vivo digital imaging in confocal microscopy. *J. Microsc.* **165(1)**, 61-69.

Robb, R. A. and Barillot, C. (1989). Interactive display and analysis of 3-D medical images. *IEEE Trans. Med. Imag.* **8**, 217-226.

Robb, R. A., Hanson, D. P., Karwoski, R. A., Larson, A. G., Workman, E. L. and Stacy, M. C. (1989). Analyze: a comprehensive, operator-interactive software package for multidimensional medical image display and analysis. *Comp. Med. Imag. Graph.* **13**, 433-454.

Rudolph, R., Vand Berg, J. and Ehrlich, H. P. (1992). Wound Contraction and Scar Contraction. In *Wound Healing: Biochemical and Clinical Aspects*, pp. 96-114. W.B. Saunders Co., Philadelphia.

Stopak, D., Wessells, N. K. and Harris, A. K. (1985). Morphogenetic rearrangement of injected collagen in developing chicken limb buds. *Proc. Nat. Acad. Sci.USA* **82**, 2804-2808.

Welch, M., Odland, G. and Clark, R. (1990). Temporal relationships of F-actin bundle formation, collagen and fibronectin matrix assembly, and fibronectin receptor expression to wound contraction. *J. Cell Biol.* **110**, 133-145.

Yang, C.-F., Crosby, C. M., Eusufzai, R. K. and Mark, R. E. (1987). Determination of paper sheet fiber orientation distributions by a laser optical difraction method. *J. Appl. Polym. Sci.* **34**, 1145-1157

.

(Received 18 August 1992 - Accepted 13 October 1992)